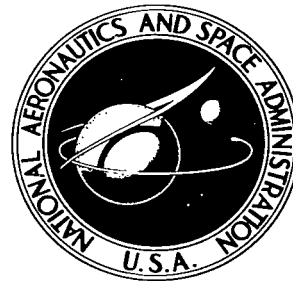


NASA TECHNICAL NOTE



NASA TN D-2604

C. I

LOAN COPY: R  
APRIL 27 1965  
KIRTLAND AFB

0079628



TECH LIBRARY KAFB, NM

NASA TN D-2604

AERODYNAMIC LOAD DISTRIBUTIONS  
FOR THE PROJECT FIRE  
CONFIGURATIONS AT MACH NUMBERS  
FROM 0.25 TO 4.63

*by Ralph J. Muraca*

*Langley Research Center*

*Langley Station, Hampton, Va.*

NASA TN D- 2604

TECH LIBRARY KAFB, NM



0079628

AERODYNAMIC LOAD DISTRIBUTIONS  
FOR THE PROJECT FIRE CONFIGURATIONS AT  
MACH NUMBERS FROM 0.25 TO 4.63

By Ralph J. Muraca

Langley Research Center  
Langley Station, Hampton, Va.

NATIONAL AERONAUTICS AND SPACE ADMINISTRATION

---

For sale by the Office of Technical Services, Department of Commerce,  
Washington, D.C. 20230 -- Price \$2.00

AERODYNAMIC LOAD DISTRIBUTIONS  
FOR THE PROJECT FIRE CONFIGURATIONS AT  
MACH NUMBERS FROM 0.25 TO 4.63

By Ralph J. Muraca  
Langley Research Center

SUMMARY

A wind-tunnel pressure-distribution study has been made to determine the aerodynamic characteristics of two cone-cylinder-frustum configurations from Mach numbers 0.248 to 4.630 over the angle-of-attack range from  $0^\circ$  to  $8^\circ$ . The results of the reduction of the tunnel pressure data to distributed normal-force derivatives, axial-force coefficients, shear-coefficient derivatives, and moment-coefficient derivatives are presented in this report. Data are analyzed in the light of linearity with angle of attack, local perturbations around discontinuities, axial-force contribution to moment coefficient, and comparison of integrated pressure data with force data from other investigations.

The results of these comparisons indicate that local nonlinearities do not appreciably affect the linearity of the total coefficients. Furthermore, for angles of attack less than  $8^\circ$ , the assumption of a linear relationship between the aerodynamic coefficients and angle of attack is valid. The axial-force contribution to the moment coefficient was found to be negligible for the model tested. The effect of a geometry change on the shear loading was found to be dependent upon Mach number.

INTRODUCTION

Project Fire is a flight reentry program being conducted by the National Aeronautics and Space Administration for the purpose of studying total heat transfer, ultra-high-temperature air radiance, materials response, and radio blackout effects at hyperbolic velocities. A standard Atlas launch vehicle is utilized in conjunction with a second stage consisting of a solid rocket motor, a reentry payload, and a short Nimbus heat shield.

In support of this program, a series of wind-tunnel tests were made to determine the aerodynamic characteristics of the Project Fire vehicle. Basic pressure distributions resulting from these tests have been published in references 1 and 2. The first tests were made by using a version of the Fire vehicle designated model I and covered a range of Mach numbers from 0.248 to 4.630 and angles of attack to  $8^\circ$ . Tests on a modified version of the vehicle, designated

as model II, were later conducted and covered a range of Mach numbers from 0.25 to 1.90 over the same angle-of-attack range.

The reduction of pressure data to the form of distributed aerodynamic data is an essential task in acquiring input for most flexible vehicle analyses. The present report presents the data of references 1 and 2 reduced to the form of distributed normal-force-coefficient slopes, axial-force coefficients, shear-coefficient slopes, and moment-coefficient slopes. In addition, the effect of angle of attack on the distributed and total aerodynamic coefficients is displayed, and a comparison of force-test data with integrated data is made. The contribution of the axial loads to the moment coefficient is also considered and the effect of this contribution presented. A secondary purpose of this paper is to present the mathematical relationships between basic pressure data and the various distributed coefficients.

#### SYMBOLS

A	surface area, in. <sup>2</sup>
F <sub>X</sub>	axial force, lb
C <sub>p</sub>	pressure coefficient, $\frac{p - p_{\infty}}{q_{\infty}}$
C <sub>m<sub>α</sub></sub>	pitching-moment-coefficient slope, radian <sup>-1</sup>
C <sub>N<sub>α</sub></sub>	normal-force-coefficient slope, radian <sup>-1</sup>
C <sub>X</sub>	axial-force coefficient
d	reference diameter, in.
F	force, lb
M <sub>X</sub>	bending moment, in-lb
F <sub>N</sub>	normal force, lb
p	local pressure, lb-in.
p <sub>∞</sub>	free-stream static pressure, lb-in. <sup>-2</sup>
q <sub>∞</sub>	free-stream dynamic pressure, lb-in. <sup>-2</sup>
r	local radius, in.
S	reference area, in. <sup>2</sup>

s            arc length, in.  
 x            distance measured along X-axis, in.  
 X,Y,Z        coordinate axes (see fig. 1)  
 $\alpha$         angle of attack ( $\alpha$  contained in ZX-plane), radians  
 $\beta$         surface slope,  $\tan \beta = \frac{dr}{dx}$ , deg  
 $\phi$         basic coordinate (see fig. 1), deg  
 Subscript:  
 l            a particular value of variable

## MODELS

The models were 0.0628 scale. Information regarding the location and number of orifices on each model, the test conditions, the procedure followed in the tests, and a description of the facilities are given in references 1 and 2. A comparison of the two configurations is shown in figure 2 and photographs of the models are shown in figures 3 and 4. The only geometrical differences between the two models occur aft of station 7.348. Model II has been lengthened by 0.650 inch and the cylindrical section has been replaced by a low-half-angle frustum-boattail combination. Station zero of model I corresponds to full-scale Atlas launch vehicle station 307.0.

## METHODS

The basic pressure data of references 1 and 2 have been integrated in accordance with the equations derived in the appendix to yield distributed loads data. As previously noted in the Introduction, the reduction of pressure data to the form of distributed aerodynamic data is an essential task in acquiring input for most flexible vehicle analyses. Although a standard notation has not yet been adopted for the distributed normal-force-coefficient slope, the advantage of the notation utilized in this report is that it can be directly incorporated into the currently popular modal-form solutions employed in the various aeroelastic analyses.

The aeroelastician is generally confronted with formulations involving linearized aerodynamics. Consequently, it is necessary that he choose representative slopes of the aerodynamic coefficients to approximate adequately the maximum aerodynamic loads to which the vehicle might be subjected. The slope of the distributed normal-force coefficient presented herein is defined as the slope of a straight line drawn through the data points obtained at an angle of attack of  $4^\circ$  or  $8^\circ$  and the origin. If the relationship between the distributed

normal-force coefficient and angle of attack were linear, these lines would be coincident.

## RESULTS AND DISCUSSION

The distributed normal-force-coefficient slope for model I is presented in table I, and representative curves are shown in figure 5. As indicated, data for angles of attack of  $4^\circ$  and  $8^\circ$  are presented. At Mach 1.470, the correlation between data taken at  $\alpha = 4^\circ$  and  $\alpha = 8^\circ$  from station 14.22 to station 24.20 was poor. This condition was attributed to the fact that at  $\alpha = 8^\circ$ , a shock wave was reflected from the tunnel walls and impinged on the aft portion of the model. Consequently, the data obtained at  $\alpha = 8^\circ$  from stations 14.22 to 24.20 have been deleted from figure 5 and all related tables. In general, the agreement between the two sets of data is good and indicates good linearity of the distributed data with angle of attack. At Mach 1.000 from stations 6.964 to 12.720 of model I, the nonlinearity with respect to the angle of attack in the range from  $4^\circ$  to  $8^\circ$  can be seen by a comparison of the data of parts (a) and (b) of table I.

The positive and negative peaks which occur in the distributed normal-force coefficient are associated with the surface discontinuities and in particular the convex corners. An examination of the appropriate pressure data reveals that just aft of the shoulders, peak negative pressure coefficients which are caused by the expansion flow around the corners occur. As angle of attack increases from  $0^\circ$ , the pressures on the windward side of the body begin slowly to increase; the pressures on the leeward side, however, increase abruptly. When these pressures are integrated, a resultant negative normal force is obtained. Farther downstream from the shoulders, similar pressure fluctuations are observed but they occur on opposite sides of the vehicle and result in positive peaks. As the Mach number is increased into the supersonic range, these peak pressure coefficients are no longer observed and, consequently, the normal-force curve does not exhibit any drastic peaks. (See fig. 5.) At present, analytical methods of predicting these peak values do not exist, and in the absence of tunnel data, the aeroelastician usually must utilize the smooth distributed data curves which are characteristic of results obtained by utilizing analytical methods. It is obvious that the requirements for an accurate determination of local loads or local flow conditions on arbitrary bodies in the lower Mach number range predicate wind-tunnel investigations.

Table II presents the distributed normal-force-coefficient slope for that portion of the Project Fire configuration which was altered. These data are presented for the Mach number range from 0.250 to 1.900. The linearity of the data is very good for all Mach numbers except 1.200. The effects of this modification on the distributed loads elsewhere on the model are not known. The data of table II are displayed in figure 6.

Although the distributed loads curve exhibits nonlinearities with respect to  $\alpha$  at local points along the model, when these data are integrated along the body length, the resultant normal loads exhibit good linearity with respect to  $\alpha$ . Table III presents the shear-coefficient slope, and representative plots

are shown in figure 7. A comparison of the total shear coefficient as defined by  $F_N/q_\infty \alpha$  of model I obtained from the data of table III shows that the ratio

$$\frac{(F_N/q_\infty \alpha)_{8^\circ}}{(F_N/q_\infty \alpha)_{4^\circ}}$$
 will vary between 0.95 and 1.10 except at Mach 1.000. The integrated data were also compared with unpublished force-test data obtained in the Langley 8-foot transonic pressure tunnel and the Langley Unitary Plan wind tunnel and the agreement was good. This comparison is shown in figure 7, where the force-test data are presented as discrete points.

A comparison of the pressures obtained along the  $\phi = 0^\circ$  meridian reveals that upstream of station 7.348, the effect on the pressure data of the configuration change from model I to model II is negligible. Thus, distributed loads curves for model II between the stations 0 and 10.126 could be obtained by combining loads data from stations 0 to 5.464 from model I with the loads data from stations 5.464 to 10.126 of model II. These combined curves were then integrated to give the shearing force at station 10.126. These results along with similar data for model I are presented in figure 8 and indicate that the shear load at station 10.126 is dependent upon the configuration for Mach  $\leq 1.470$ . For Mach  $> 1.470$ , the configuration change has little effect on the shear load.

The  $r \tan \beta$  contribution to the integral of the moment coefficient slope equation given in the appendix frequently is ignored in computing the moments and centers of pressure on slender bodies. Often, wind-tunnel data will show the center of pressure for a low-fineness-ratio body to lie entirely outside the geometrical boundaries of the body. A principal factor in causing this condition is the axial-force component of the moment coefficient. The axial-force component is inversely proportional to the fineness ratio of the body, and for low-fineness-ratio configurations can result in a significant shift in the location of the center of pressure. In table IV, the moment-coefficient derivative  $M_X/q_\infty \alpha$  including the axial-force component mentioned above is presented for angles of attack of  $4^\circ$  and  $8^\circ$ . Representative curves are shown in figure 9. It is emphasized that the moment defined by the moment coefficient slope equation in the appendix is about the diametrical axis normal to the XZ plane in which angle of attack is measured. Figure 10 is a comparison of this equation with and without the effect of the  $r \tan \beta$  term. The effect of the axial-force component is to reduce the net moment. Mach 1.000 data were used since this case was found to be the one with the greatest variation. The error introduced by deleting the axial-force component in the moment equation is graphically displayed on the figure and is small for this configuration.

The axial-force coefficient  $F_X/q_\infty$  obtained from  $\alpha = 0^\circ$  data is shown in table V and representative curves are shown in figure 11. For a given free-stream dynamic pressure  $q_\infty$  it yields the external axial force acting on the body at any station. It should be noted, however, that this is the resultant axial load of the externally applied pressure forces and does not include viscous effects.

## CONCLUDING REMARKS

In general, the assumption of a linear relationship between normal force and angle of attack for angles of attack less than  $8^{\circ}$  will yield results which are within the limits of accuracy acceptable in many types of analyses. Although local nonlinearities occur in the distributed loads data, their effect on the overall normal force is insignificant for the model investigated. The effect of a major geometrical variation on the normal or shear force downstream of the changed section was slight for Mach numbers greater than 1.470. For Mach number less than or equal to 1.470, the shear loads are dependent on the configuration shape. Ignoring the axial-force contribution to the bending moment introduced little error for the model tested. As the fineness ratio is decreased, however, this error will increase.

Langley Research Center,  
National Aeronautics and Space Administration,  
Langley Station, Hampton, Va., October 9, 1964.

## APPENDIX

### ANALYSIS

The basic equations essential for the reduction of wind-tunnel pressure data to the distributed normal-force derivative  $\frac{dC_{N\alpha}}{dx} S$ , the distributed axial-force coefficient  $\frac{dC_X}{dx} S$ , the shear-coefficient derivative,  $\frac{F_N}{q_\infty \alpha}$ , and the moment-coefficient derivative  $C_m \alpha S d$  are derived as follows: In figure 1, the basic coordinates necessary to the analytics are shown for a volume of revolution generated about its OX axis. The ZY plane is considered normal to the OX axis, and the angle of attack of the airstream is assumed to lie in the XZ plane. A differential force  $dF$  is shown to result from the local pressure and to act normal to the surface of the element  $dA$ . Viscous forces are not considered. The normal and axial forces resulting from the pressure on the body surface are given by

$$F_N = - \int_{\sigma} dF \cos \beta \cos \phi \quad (1)$$

and

$$F_X = \int_{\sigma} dF \sin \beta \quad (2)$$

where  $\int_{\sigma}$  indicates integration over the body surface.

The expression for  $dF$  can be written in terms of the local pressure  $p$  as

$$dF = p dA \quad (3)$$

and, if the higher order products of differentials are ignored, then

$$dA = r \sec \beta d\phi dx \quad (4)$$

Substituting equations (3) and (4) into equations (1) and (2) and introducing the dummy variable  $\lambda$  yields

$$F_N = - \int_0^x \int_0^{2\pi} pr \cos \phi d\phi d\lambda \quad (5)$$

and

$$F_X = \int_0^x \int_0^{2\pi} pr \tan \beta d\phi d\lambda \quad (6)$$

Differentiating with respect to  $x$  gives

$$\frac{dF_N}{dx} = - \int_0^{2\pi} pr \cos \phi d\phi \quad (7)$$

$$\frac{dF_X}{dx} = \int_0^{2\pi} pr \tan \beta d\phi \quad (8)$$

If the distributed coefficients are defined as follows:

$$\left( S \frac{dC_{N\alpha}}{dx} \right) = \frac{1}{q_\infty^\alpha} \frac{dF_N}{dx} \quad (9)$$

$$\left( S \frac{dC_X}{dx} \right) = \frac{1}{q_\infty} \frac{dF_X}{dx} \quad (10)$$

substitution of equations (7) and (8) into equations (9) and (10) yields

$$\left( S \frac{dC_{N\alpha}}{dx} \right) = - \frac{1}{q_\infty^\alpha} \int_0^{2\pi} pr \cos \phi d\phi \quad (11)$$

$$\left( S \frac{dC_X}{dx} \right) = \frac{1}{q_\infty} \int_0^{2\pi} pr \tan \beta d\phi \quad (12)$$

The pressure term is defined as

$$p = p_\infty + C_p q_\infty \quad (13)$$

Simplifying the substitution of equation (13) into equations (11) and (12) yields

$$\left( S \frac{dC_{N\alpha}}{dx} \right) = - r \int_0^{2\pi} \frac{C_p}{\alpha_t} \cos \phi \, d\phi \quad (14)$$

and

$$\left( S \frac{dC_X}{dx} \right) = \frac{r \tan \beta}{q_\infty} \int_0^{2\pi} (p_\infty + q_\infty C_p) d\phi \quad (15)$$

where the subscript  $t$  has been added to  $\alpha$  to signify the test angle of attack.

If the axial force is obtained from  $\alpha_t = 0$  data,

$$\left( S \frac{dC_X}{dx} \right) = 2\pi r \left( \frac{p}{q_\infty} \right) \tan \beta \quad (16)$$

Integrating equation (16) over the interval  $(0, x_1)$  and multiplying by  $q_\infty$  gives

$$F_{X_1} = 2\pi \int_0^{x_1} pr \tan \beta \, dx \quad (17)$$

The normal-force-coefficient slope is given by integrating equation (14) over the interval  $(0, x_1)$ , that is,

$$\frac{F_{N_1}}{q_\infty \alpha_1} = - \int_{x=0}^{x_1} r \int_{\phi=0}^{2\pi} \frac{C_p}{\alpha_t} \cos \phi \, d\phi \, dx \quad (18)$$

Note that the  $\alpha_t$  under the integral is retained in order to maintain a general form that can accommodate pressure data that have been obtained with varying angles of attack with the orientation angle  $\phi$ . Furthermore, the shear-coefficient derivative for the configuration between  $x = 0$  and  $x = x_1$  is given by

$$C_{N\alpha} S \Big|_0^{x_1} = - \int_{x=0}^{x_1} r \int_0^{2\pi} \frac{C_p}{\alpha_t} \cos \phi \, d\phi \, dx \quad (19)$$

The moment-coefficient slope about  $x = x_1$  resulting from the normal and axial forces acting on the body between  $x = 0$  and  $x = x_1$  at an angle of attack  $\alpha_1$  is

$$\frac{M_{X_1}}{q_\infty \alpha_1} = \int_{x=0}^{x_1} r(x - x_1 + r \tan \beta) \int_{\phi=0}^{2\pi} \frac{C_p}{\alpha_t} \cos \phi d\phi dx \quad (20)$$

Substituting equation (14) into equation (20) yields the moment-coefficient-slope equation in terms of the distributed normal-force derivative

$$\frac{M_{X_1}}{q_\infty \alpha_1} = \int_{x=0}^{x_1} (x_1 - x - r \tan \beta) \frac{dC_{N\alpha}}{dx} S dx \quad (21)$$

In evaluating the integral of equation (21), it should be noted that in most practical applications,  $\tan \beta = \infty$  when  $x = 0$ . However, the limit of  $r \tan \beta$  as  $x \rightarrow 0$  is finite; thus, the singularity will not be present when dealing numerically with the product  $r \tan \beta$ . Defining the moment-coefficient derivative as

$$C_{m\alpha} S_d = \frac{M_{X_1}}{q_\infty \alpha} \quad (22)$$

where  $d$  is a reference diameter yields

$$C_{m\alpha} S_d \Big|_0^{x_1} = \int_{x=0}^{x_1} (x_1 - x - r \tan \beta) \frac{dC_{N\alpha}}{dx} S dx \quad (23)$$

#### REFERENCES

1. Henderson, William P.: Pressure Distributions Over the Forward Portion of the Project Fire Space-Vehicle Configuration at Mach Numbers From 0.25 to 0.60. NASA TN D-1612, 1963.
2. Pearson, Albin O.: Surface Pressure Distributions on 0.0628-Scale Models of Proposed Project Fire Space Vehicles at Mach Numbers From 0.25 to 4.63. NASA TN D-1961, 1963.

TABLE I.- DISTRIBUTED NORMAL-FORCE-COEFFICIENT SLOPE FOR MODEL I

(a)  $\alpha = 4^\circ$ 

Model stations, x, in.	$S \frac{dc_{N\alpha}}{dx}$ , in./radian, for -										
	M = 0.248	M = 0.395	M = 0.585	M = 0.800	M = 1.000	M = 1.200	M = 1.470	M = 1.900	M = 2.700	M = 3.400	M = 4.630
0.000	0.0000	0.0000	0.0000	0.0000	0.0000	0.0000	0.0000	0.0000	0.0000	0.0000	0.0000
.125	3.0964	3.1071	3.1246	2.7779	2.3663	1.9038	1.8347	1.9195	1.8746	1.6020	2.3653
.250	4.3107	4.5737	4.7087	4.6858	3.8267	2.7168	2.7109	2.6441	2.5088	2.1546	2.7555
.500	3.2791	3.5973	3.8075	4.1328	6.2831	4.6164	3.2931	2.6651	2.1538	1.8347	2.1588
1.000	2.6896	2.8165	2.8711	2.7278	2.4861	4.9838	3.6187	3.1279	2.4018	1.8698	2.0240
1.500	2.8793	3.3430	2.9179	2.6041	2.3878	1.5267	3.1273	3.0653	2.6270	2.0755	2.1308
2.000	2.9984	3.2398	3.2648	3.1073	2.9481	2.5576	2.5814	3.2143	2.9710	2.3848	2.5211
2.500	3.3965	3.5917	3.6434	3.5832	3.4178	3.3053	2.7672	3.3904	3.2850	2.7542	2.9523
3.500	3.8137	4.2113	4.3495	4.4553	4.2254	4.0439	3.5457	4.1569	4.1190	3.7487	4.1128
4.500	4.9609	4.9372	4.9662	4.2623	4.6713	5.5971	4.4438	4.7884	5.0029	4.8229	5.4115
5.000	4.0623	4.6816	5.0674	4.4561	3.5253	3.7338	4.3670	5.2259	5.2882	4.8086	5.1240
5.250	4.5607	4.6584	5.1722	4.6592	4.3128	4.5844	4.4976	5.2845	5.6871	5.5701	6.3040
5.714	-5.8427	3.2388	3.2305	-1.6335	2.5442	2.0490	2.3647	3.0021	2.6754	2.4228	2.5498
5.964	2.9501	2.3262	2.1648	5.5192	3.4409	2.5671	2.6656	3.0024	2.5647	2.1323	2.1441
6.464	.8139	.9013	.8989	4.1092	-2.6222	3.4523	2.7521	2.9511	2.3474	1.7465	1.7011
6.964	-.2361	.0710	.1393	-.9616	-17.0306	3.9133	2.5556	2.5296	2.3474	1.6668	1.5864
7.598	-2.7493	-2.4370	-2.3944	-2.4509	-1.6057	-1.5180	-1.1921	.0129	.2966	-.2659	-.3149
7.848	-2.0232	-2.1097	-2.4281	-4.8301	-1.3100	1.8391	.7991	.6838	.2870	-.2771	-.2528
8.348	4.4570	5.2206	4.2426	.9752	-1.2144	4.1786	2.4390	2.2177	2.4364	.3144	.0111
8.848	.7734	1.9440	2.6955	2.0456	-.3693	1.9281	1.3218	1.5253	1.8713	1.3637	.3931
9.348	.4959	1.0602	1.4195	1.7846	1.4975	-1.5879	.8635	1.1625	1.5525	1.6505	.6898
9.848	1.2372	1.7759	1.9681	2.5753	4.5558	-4.8386	-1.4990	1.0820	1.6308	1.8919	1.1853
10.376	1.7971	2.5238	2.7605	3.7576	9.1555	3.7414	1.4397	1.7523	2.7724	2.5381	1.6822
10.626	1.7290	2.1336	2.2029	3.0123	11.7994	2.7001	.9052	1.4561	2.7822	3.1240	2.4180
11.126	2.0394	2.5566	2.7052	3.3110	13.8821	2.2748	.6080	1.4344	2.8580	3.3001	3.5662
11.626	2.4813	3.1066	3.1969	3.5365	11.9470	2.4226	1.0167	1.9608	3.1849	3.6364	4.0414
12.126	3.1540	3.3341	3.6335	3.7869	8.6504	2.4394	1.1884	2.1833	3.3438	3.8416	4.5847
12.720	3.3449	3.8525	4.0308	4.3225	5.9617	3.0897	1.3957	2.2439	3.4371	4.0147	4.6453
13.220	3.1259	4.1261	4.3620	4.6329	4.5716	3.5817	1.8804	2.5869	3.7392	4.1615	4.8934
14.220	3.6652	4.5223	4.8699	5.2132	3.8090	4.3221	2.8546	2.9131	3.8644	4.1598	5.0406
15.220	4.2177	4.9132	5.3674	5.5967	3.9699	4.7779	4.1098	3.5492	4.1885	4.3260	5.1974
16.220	4.7920	5.4263	5.9093	6.3934	5.2076	6.0209	5.1099	4.2575	4.5982	4.7359	4.5046
17.220	5.0972	5.8619	6.2665	6.8132	5.9823	6.5639	6.0479	4.7885	5.0641	5.1582	5.7808
18.220	5.2776	5.9896	6.4940	7.2620	6.7017	6.5583	6.7126	5.2059	5.4673	5.3788	6.0854
19.220	5.0524	6.0515	6.6692	7.8334	7.5404	6.9546	7.4065	5.5487	5.9099	5.6272	6.0745
20.220	4.7739	6.0029	6.6103	8.5472	8.6688	6.8657	7.5009	5.9266	6.2582	5.9463	6.2334
20.720	4.4071	5.6693	6.5157	9.2955	9.8694	8.3448	7.7649	6.1435	6.4364	6.1518	6.2598
21.450	1.7846	2.7907	2.9350	.2841	5.9922	5.4688	5.2861	3.7295	3.2684	2.8381	2.7060
21.700	2.6079	3.2986	3.4580	-16.9249	5.3959	4.6683	4.5928	3.5568	2.7440	2.3514	2.3342
22.200	2.3838	2.9236	3.0672	3.8066	3.9708	4.2707	4.4433	3.4821	2.4823	1.8382	1.9690
23.200	1.5326	2.8047	2.7019	2.5134	4.1981	4.8071	3.9611	3.6003	2.9270	1.8118	1.5822
24.200	2.1872	2.9138	2.7212	2.5769	4.2545	4.3921	3.2195	3.4814	3.1113	1.9212	1.4988

TABLE I.- DISTRIBUTED NORMAL-FORCE-COEFFICIENT SLOPE FOR MODEL I - Concluded

(b)  $\alpha = 8^\circ$ 

Model stations, x, in.	$S \frac{dC_{N\alpha}}{dx}$ , in./radian, for -											
	M = 0.248	M = 0.395	M = 0.585	M = 0.800	M = 1.000	M = 1.200	M = 1.470	M = 1.900	M = 2.700	M = 3.400	M = 4.630	
0.000	0.0000	0.0000	0.0000	0.0000	0.0000	0.0000	0.0000	0.0000	0.0000	0.0000	0.0000	
.125	2.8914	3.0564	3.0170	2.7756	2.3255	1.9533	1.8065	1.8234	1.8117	1.7903	1.8302	
.250	4.1726	4.4524	4.5054	4.6014	3.8121	2.9187	2.5550	2.5412	2.4778	2.4007	2.4407	
.500	3.3451	3.6185	3.7568	3.8925	5.7190	4.8999	3.2595	2.6871	2.2220	2.0012	1.8973	
1.000	2.5792	2.7564	2.7168	2.7246	2.3398	4.2569	3.5521	3.0737	2.3512	2.0325	1.8685	
1.500	2.7124	2.9493	2.8155	2.8831	2.5703	2.3889	3.0878	3.1380	2.5717	2.2583	2.0839	
2.000	2.8553	3.0754	3.1093	3.1495	2.9443	2.5676	2.8212	3.3036	2.9017	2.6303	2.4345	
2.500	3.2265	3.4476	3.4225	3.5654	3.3810	3.2823	2.9285	3.5667	3.2369	3.0237	2.8931	
3.500	3.8155	4.0500	4.1413	4.3244	4.1265	4.2749	3.7602	4.2700	4.2147	4.1040	4.1070	
4.500	4.3966	4.8781	4.7424	5.0043	4.4542	4.3533	4.5628	5.1728	5.2483	5.2329	5.3330	
5.000	3.9649	4.5502	4.7040	4.6352	3.4789	3.6887	4.7250	5.5107	5.5349	5.2526	4.9902	
5.250	4.2031	4.5640	4.8578	4.4741	4.1319	4.4732	4.9821	5.6871	5.7015	5.8605	6.2283	
5.714	-.3885	4.1878	3.2525	-7.4702	2.4506	2.0879	2.6273	3.0476	2.7359	2.5301	2.4877	
5.964	2.4847	2.2511	2.0104	4.9514	3.3693	2.6360	2.8160	3.0531	2.5501	2.2720	2.0058	
6.464	1.0172	1.0041	.8434	3.9257	-2.4042	3.5213	2.8426	2.9872	2.3376	1.9877	1.7256	
6.964	.1648	.0704	-.0251	-.2087	-5.9675	3.9421	2.6549	2.9155	2.2956	1.9066	1.5752	
7.598	-2.0382	-2.2951	-2.1361	-2.7311	-2.5496	-2.1851	-1.0609	.0024	.3573	.1573	.0400	
7.848	-.9217	-1.5517	-1.9546	-3.6421	-2.2879	.7875	1.3641	1.9972	.6708	.4828	.1093	
8.348	3.3430	4.2734	4.0660	1.9392	-.7545	3.4704	2.6056	2.4568	2.1509	1.6318	.8283	
8.848	1.0322	1.4697	1.9069	2.0001	1.4525	1.7384	1.5376	1.8640	1.8581	1.5693	.9836	
9.348	1.0282	1.0151	1.1473	1.7963	3.8115	-.2498	.7011	1.6569	1.8043	1.4976	1.0817	
9.848	1.5855	1.6880	1.8290	2.4716	6.3024	-1.7957	-1.2061	1.0963	1.8186	1.4172	1.3834	
10.376	2.2589	2.3675	2.4112	3.6323	8.0964	4.3836	1.9976	2.3671	3.0157	2.4242	1.9676	
10.626	2.1006	2.1940	2.2117	2.8995	7.9913	3.0434	1.5208	2.1205	2.9825	2.6992	2.5468	
11.126	2.4977	2.4876	2.6391	3.1667	6.6544	2.4826	1.1578	2.0193	3.0434	2.9638	3.3255	
11.626	2.8977	2.9811	3.0831	3.4921	5.0839	2.5937	1.5307	2.3228	3.3551	3.2846	3.8754	
12.126	3.1433	3.3358	3.4087	3.7357	4.1679	2.6047	1.6540	2.4544	3.5131	3.5203	4.1819	
12.720	3.5619	3.8077	3.8888	4.2300	4.2779	3.1080	1.9463	2.5653	3.6433	3.7151	4.5353	
13.220	3.9353	4.0555	4.2113	4.5596	4.4989	3.4221	2.4697	2.8282	3.9158	3.8954	4.7704	
14.220	4.2778	4.3929	4.6294	5.1143	4.9362	4.1881	3.0584	3.1546	4.0761	3.9897	4.8877	
15.220	4.5097	4.7352	4.9878	5.5021	5.3868	4.9406	3.7653	3.6605	4.4711	4.2741	5.1207	
16.220	4.9712	5.2404	5.5328	6.2182	6.2942	5.8424		4.2251	4.9280	4.6293	5.4223	
17.220	5.2460	5.4410	5.8039	6.6339	6.7269	6.3662		4.6348	5.3416	4.9777	5.7342	
18.220	5.4039	5.6476	5.9696	6.9926	7.0965	6.6997		5.0572	5.7025	5.2234	5.8872	
19.220	5.6901	5.6051	6.1328	7.5568	7.5081	7.0595		5.4491	6.1176	5.4931	6.0580	
20.220	5.0622	5.4722	6.0309	8.0033	7.5756	7.4155		5.8936	6.3135	5.7394	6.4003	
20.720	4.7182	5.1288	5.7207	8.5355	8.1036	8.5255		6.0871	6.3783	5.8147	6.5389	
21.450	2.5609	2.5931	2.6836	-3.2587	4.8976	4.9973		3.4966	3.4612	2.8169	3.4550	
21.700	3.1082	2.7755	2.9874	-3.2594	4.9651	4.5843		3.4224	3.1009	2.5878	3.1397	
22.200	2.4568	2.3233	2.5547	2.8861	5.1730	4.3570		3.5444	3.0594	2.3814	2.7843	
23.200	1.9703	1.8224	2.0257	1.6515	6.5524	5.0821		3.5579	3.2156	2.4244	2.5534	
24.200	1.7518	1.2982	1.6191	1.3798	6.6239	4.7998		3.3858	3.1760	2.4907	2.3964	

TABLE II.- DISTRIBUTED NORMAL-FORCE-COEFFICIENT SLOPE FOR MODEL II

(a)  $\alpha = 4^\circ$ 

Model stations, x, in.	$S \frac{dC_{N\alpha}}{dx}$ , in./radian, for -								
	M = 0.250	M = 0.400	M = 0.600	M = 0.800	M = 1.000	M = 1.200	M = 1.470	M = 1.600	M = 1.900
7.348	-1.2658	-0.9429	-1.1850	-1.9532	-6.0193	-1.1918	-----	-----	-----
7.473	-1.1832	-1.1391	-1.3050	-1.8963	-5.6034	-1.2691	-1.3604	-1.2453	-0.8388
7.598	-1.7017	-1.3000	-1.6047	-2.7407	-5.5312	-1.4887	-1.5106	-1.4422	-.8072
7.848	-----	1.3237	.2420	-1.0768	-4.4503	1.3652	2.0655	1.9587	1.7609
8.348	2.1856	2.9328	2.9762	2.8163	1.0873	.4513	4.6376	4.2430	3.7778
8.929	-3.3656	-3.7412	-4.7388	-1.6536	-5.5077	4.3825	3.5340	3.3590	2.8830
9.179	-1.0425	-.8772	-1.5329	-3.0221	-2.7712	1.5892	1.5476	1.5250	1.3098
9.429	-----	-.3095	-.9810	-1.7252	-.0611	1.0894	1.4982	1.3860	1.1807
9.929	-----	.17699	-.3243	-.2924	4.7191	-.1146	.80356	1.0220	.98806
10.429	.9649	1.6986	1.4422	2.0076	1.0668	-1.6059	-.96632	-4.1700	.40782
10.776	3.6969	4.5558	4.4108	4.1912	2.5396	2.0417	1.1639	.90085	.34424
11.026	-----	2.8268	2.9051	3.5601	2.5880	4.2530	2.8667	2.5090	2.1979
11.276	1.7440	1.9889	2.0628	2.7249	1.4747	3.7116	2.3293	2.0608	1.8518
11.776	1.6823	2.0018	1.9384	2.2648	5.0191	1.3551	1.3804	1.3037	1.7514
12.276	-----	2.4981	2.5132	2.8255	3.8375	1.6918	.60184	.95069	1.6604
12.870	2.9565	3.4639	3.4825	3.8754	4.1907	4.3697	2.9817	2.4885	2.0013

(b)  $\alpha = 8^\circ$ 

Model stations, x, in.	$S \frac{dC_{N\alpha}}{dx}$ , in./radian, for -								
	M = 0.250	M = 0.400	M = 0.600	M = 0.800	M = 1.000	M = 1.200	M = 1.470	M = 1.600	M = 1.900
7.348	-1.0218	-0.71703	-0.83532	-0.96627	-4.2477	-1.1308	-----	-----	-----
7.473	-1.1659	-.99076	-1.0472	-1.0986	-3.8510	-1.1865	-1.4242	-1.0745	-0.70052
7.598	-1.7941	-1.5215	-1.3846	-1.7886	-3.8054	-1.4580	-1.6253	-1.2281	-.72280
7.848	-----	2.1000	1.0624	.60316	-2.9872	1.7375	2.5177	2.8378	2.4211
8.348	2.0477	2.4175	2.9858	3.4527	2.3875	.4475	4.3630	4.5095	3.5713
8.929	-3.0236	-2.9252	-4.0137	-1.0886	-.25237	3.8654	2.9392	3.3418	2.6647
9.179	-.67725	-.61895	-1.0087	-2.5970	-2.2562	1.1956	1.2983	1.6344	1.2906
9.429	-----	-.19687	-.48893	-1.3696	.51011	.92939	1.2077	1.5606	1.2755
9.929	-----	.36446	.13162	.14675	5.0003	-6.0428	.40184	1.0633	1.0488
10.429	1.2297	1.6580	1.6827	2.2404	.34326	-6.1508	-4.6463	-3.0422	-.98244
10.776	3.3382	3.7260	4.1398	4.3583	1.3936	2.4485	1.0353	1.4689	.81845
11.026	-----	2.6784	2.9891	3.6480	.89546	4.1810	2.3241	2.7626	2.1678
11.276	1.7773	2.1243	2.3834	2.9712	5.8950	3.6096	1.8523	2.3926	1.9383
11.776	1.8757	2.2296	2.2845	2.6642	3.7501	1.7458	1.0075	1.8778	1.7720
12.276	2.8060	2.8194	3.0563	3.1231	2.0066	.60368	1.5231	1.6434	1.2243
12.870	3.0899	3.5480	3.6896	3.9960	3.5916	3.9982	2.4262	2.8821	2.2243

TABLE III.- SHEAR-COEFFICIENT SLOPE FOR MODEL I

(a)  $\alpha = 4^\circ$ 

Model stations, x, in.	$\frac{F_N}{q_{\infty} \alpha}$ , in. <sup>2</sup> /radian, for -											
	M = 0.248	M = 0.395	M = 0.585	M = 0.800	M = 1.000	M = 1.200	M = 1.470	M = 1.900	M = 2.700	M = 3.400	M = 4.630	
0.000	0.00000	0.00000	0.00000	0.00000	0.00000	0.00000	0.00000	0.00000	0.00000	0.00000	0.00000	
.125	.19332	.19399	.19508	.17343	.14773	.11885	.11454	.11984	.11704	.10002	.14768	
.250	.65577	.67354	.68415	.63942	.53439	.40733	.39834	.40476	.39071	.33455	.46739	
.500	1.6035	1.6938	1.7476	1.7406	1.7968	1.3230	1.1481	1.0677	.97292	.83269	1.0810	
1.000	3.0941	3.2956	3.4155	3.4539	3.9868	3.7206	2.8742	2.5144	2.1106	1.7578	2.1256	
1.500	4.4849	4.8359	4.8612	4.7855	5.2040	5.3465	4.5589	4.0611	3.3665	2.7431	3.1633	
2.000	5.9528	6.4779	6.4053	6.2119	6.5366	6.3665	5.9846	5.6294	4.7646	3.8570	4.3250	
2.500	7.5498	8.1839	8.1305	7.8828	8.1264	7.8307	7.3204	7.7288	6.3269	5.1404	5.6919	
3.500	11.151	12.081	12.123	11.898	11.944	11.501	10.474	11.049	10.025	8.3885	9.2208	
4.500	15.554	16.651	16.776	16.252	16.388	16.317	14.464	15.517	14.581	12.670	13.978	
5.000	17.787	19.053	19.282	18.429	18.435	18.647	16.664	18.017	17.151	15.075	16.609	
5.250	18.864	20.219	20.560	19.568	19.413	19.686	17.771	19.330	18.522	16.371	18.036	
5.714	18.567	22.050	22.508	20.269	21.003	21.223	19.362	21.250	20.460	18.224	20.088	
5.964	18.206	22.744	23.181	20.754	21.750	21.800	19.990	22.000	21.114	18.792	20.674	
6.464	19.146	23.550	23.946	23.159	21.954	23.303	21.343	23.487	22.341	19.761	21.634	
6.964	19.290	23.793	24.136	23.945	17.046	25.142	22.668	24.856	23.513	20.613	22.455	
7.598	18.345	23.044	23.334	22.864	11.145	25.901	23.100	25.661	24.351	21.057	22.858	
7.848	17.749	22.476	22.732	21.955	10.781	25.941	23.051	25.748	24.424	20.989	22.787	
8.348	18.357	23.253	23.185	20.992	10.150	27.444	23.860	26.472	25.104	20.999	22.727	
8.848	19.663	25.042	24.917	21.747	9.7548	28.969	24.799	27.407	26.179	21.418	22.828	
9.348	19.980	25.793	25.945	22.703	10.037	29.054	25.345	28.078	27.035	22.170	23.098	
9.848	20.413	26.501	26.791	23.792	11.548	27.449	25.186	28.639	27.830	23.055	23.567	
10.376	21.213	27.635	28.038	25.462	15.163	27.160	25.170	29.386	28.991	24.223	24.323	
10.626	21.653	28.217	28.658	26.307	17.780	27.964	25.463	29.787	29.684	24.930	24.835	
11.126	22.594	29.388	29.884	27.887	24.194	29.206	25.841	30.059	31.093	26.535	26.329	
11.626	23.723	30.802	31.358	29.597	30.644	30.379	26.247	31.357	32.602	28.267	28.229	
12.126	25.131	32.411	33.063	31.426	35.788	21.594	26.798	32.392	34.233	30.135	30.383	
12.720	27.059	34.543	35.337	33.832	40.123	33.234	27.564	33.705	36.244	32.466	33.122	
13.220	28.675	36.535	37.433	36.068	42.754	34.900	28.382	34.912	38.037	34.507	35.504	
14.220	32.067	40.855	42.044	40.986	46.940	38.838	30.747	37.659	41.834	38.664	40.466	
15.220	36.004	45.568	47.158	46.385	50.825	43.393	34.226	40.887	45.857	42.902	45.579	
16.220	40.504	50.732	52.790	52.374	55.409	48.787	38.831	44.786	50.245	47.428	50.925	
17.220	45.444	56.370	58.872	58.971	60.998	55.073	44.404	49.304	55.071	52.370	56.562	
18.220	50.626	62.290	65.245	66.001	67.334	61.627	50.778	54.296	60.332	57.633	62.489	
19.220	55.785	68.304	71.820	73.541	74.447	68.376	57.830	59.668	66.014	63.131	68.562	
20.220	60.693	74.325	78.453	81.722	82.543	75.279	65.276	65.400	72.092	68.911	74.710	
20.720	62.986	77.240	81.731	86.178	87.173	79.078	69.088	68.414	75.262	71.933	77.830	
21.450	65.244	80.235	85.177	89.669	92.956	84.115	73.847	72.014	78.801	75.210	81.099	
21.700	65.792	81.085	85.975	87.591	94.378	85.381	75.080	72.924	79.552	75.858	81.728	
22.200	67.059	82.639	87.605	84.315	96.718	87.613	77.337	74.681	80.857	76.905	82.803	
23.200	68.995	85.500	90.486	87.472	100.800	92.147	81.535	78.219	83.559	78.728	84.577	
24.200	70.853	88.357	93.195	90.014	105.020	96.742	85.121	81.756	86.575	80.592	86.116	

TABLE III.- SHEAR-COEFFICIENT SLOPE FOR MODEL I - Concluded

(b)  $\alpha = 8^\circ$ 

Model stations, x, in.	$\frac{F_N}{q_{\infty} \alpha}$ , in. <sup>2</sup> /radian, for -										
	M = 0.248	M = 0.395	M = 0.585	M = 0.800	M = 1.000	M = 1.200	M = 1.470	M = 1.900	M = 2.700	M = 3.44	M = 4.630
0.000	0.00000	0.00000	0.00000	0.00000	0.00000	0.00000	0.00000	0.00000	0.00000	0.00000	0.00000
.125	.18052	.19082	.18836	.17329	.14518	.12195	.11278	.11384	.11311	.11177	.11426
.250	.62156	.65963	.65802	.63387	.52839	.42613	.38509	.38634	.38092	.37343	.38091
.500	1.5603	1.6674	1.6897	1.6945	1.7185	1.4024	1.1111	1.0392	.96778	.92308	.92259
1.000	3.0398	3.2545	3.3064	3.3470	3.7311	3.6892	2.8123	2.4780	2.1099	1.9305	1.8631
1.500	4.3613	4.6744	4.6880	4.7475	4.9574	5.3490	4.4705	4.0292	3.3393	3.0020	2.8501
2.000	5.7518	6.1790	6.1677	6.2541	6.3346	6.5868	5.9462	5.6379	4.7062	4.2229	3.9785
2.500	7.2707	7.8081	7.8014	7.9310	7.9142	8.0477	7.3821	7.3537	6.2393	5.6349	5.3091
3.500	10.788	11.553	11.584	11.871	11.664	11.822	10.723	11.267	9.9612	9.1950	8.8054
4.500	14.889	16.012	16.021	16.531	15.949	16.132	14.880	15.984	14.687	13.859	13.521
5.000	16.978	18.362	18.380	18.938	17.931	18.140	17.199	18.652	17.380	16.477	16.099
5.250	17.998	19.497	19.574	20.076	18.881	19.159	18.411	20.050	18.873	17.865	17.499
5.714	18.881	21.535	21.454	19.381	20.407	20.680	20.175	22.075	20.739	19.810	19.519
5.964	19.144	22.329	22.111	19.067	21.133	21.270	20.855	22.836	21.399	20.409	20.081
6.464	20.019	23.142	22.824	21.284	21.374	22.807	22.268	24.345	22.619	21.473	21.012
6.964	20.313	23.411	23.028	22.212	19.284	24.671	23.641	25.819	23.777	22.446	21.837
7.598	19.720	22.706	22.344	21.281	16.586	25.228	24.145	26.743	24.617	23.099	22.348
7.848	19.351	22.228	21.833	20.845	15.982	25.053	24.183	26.993	24.745	23.179	22.367
8.348	19.955	22.913	22.360	20.060	15.223	26.116	25.175	28.105	25.450	23.707	22.601
8.848	21.048	24.347	23.852	21.094	15.397	27.417	26.209	29.185	26.451	24.507	23.054
9.348	21.562	24.968	24.615	22.092	16.712	27.789	26.768	30.063	27.366	25.272	23.569
9.848	22.215	25.643	25.358	23.158	19.237	27.278	26.642	30.751	28.270	26.000	24.185
10.376	23.229	26.712	26.476	24.767	23.035	27.961	26.851	31.664	29.545	27.013	25.069
10.626	23.773	27.282	27.053	25.583	25.044	28.888	27.290	32.225	30.294	27.653	25.632
11.126	24.921	28.451	28.265	27.098	28.701	30.268	27.959	33.259	31.799	29.067	27.099
11.626	26.269	29.817	29.694	28.761	31.633	31.536	28.631	34.343	33.392	30.268	28.897
12.126	27.778	31.395	31.315	30.566	33.943	32.834	29.426	35.536	35.102	32.327	30.909
12.720	29.767	33.514	33.480	32.929	36.449	34.529	30.494	37.025	37.226	34.474	33.496
13.220	31.640	35.478	35.503	35.124	38.641	36.160	31.597	38.372	39.113	36.375	35.820
14.220	35.741	39.697	39.919	39.956	43.354	39.961	34.358	41.361	43.105	40.313	40.644
15.220	40.131	44.257	44.722	45.259	48.510	44.520	37.767	44.765	47.374	44.441	45.643
16.220	44.866	49.239	49.977	51.113	54.344	49.906		48.803	52.069	48.888	50.909
17.220	49.969	54.574	55.640	57.532	60.848	56.005		53.129	57.198	53.686	56.481
18.220	55.289	60.113	61.520	64.338	67.752	62.331		57.969	62.715	58.781	62.286
19.220	60.830	65.733	67.565	71.606	75.047	69.403		63.217	68.619	64.134	68.252
20.220	66.220	71.266	73.641	79.377	82.581	76.633		68.883	74.828	69.744	74.475
20.720	68.643	73.914	76.575	83.508	86.497	80.614		71.875	77.997	72.630	77.706
21.450	71.297	76.729	79.636	85.432	91.237	85.544		75.369	81.585	75.777	81.350
21.700	72.005	77.400	80.348	84.618	92.469	86.741		76.233	82.404	76.452	82.174
22.200	73.395	78.673	81.732	84.525	95.000	88.974		77.973	83.943	77.693	83.653
23.200	75.606	80.744	84.020	86.791	100.857	93.689		81.251	87.077	80.093	86.319
24.200	77.465	82.302	85.840	88.305	107.438	98.624		84.989	90.269	82.548	88.791

TABLE IV.- MOMENT-COEFFICIENT SLOPE FOR MODEL I

(a)  $\alpha = 4^\circ$ 

Model stations, x, in.	$\frac{M_X}{q_\infty \alpha}$ , in. <sup>3</sup> /radian, for -											
	M = 0.248	M = 0.395	M = 0.585	M = 0.800	M = 1.000	M = 1.200	M = 1.470	M = 1.900	M = 2.700	M = 3.400	M = 4.630	
0.000	0.000	0.000	0.000	0.000	0.000	0.000	0.000	0.000	0.000	0.000	0.000	0.000
.125	-.115	-.116	-.116	-.104	-.088	-.071	-.068	-.072	-.070	-.060	-.088	
.250	-.309	-.318	-.323	-.302	-.252	-.192	-.188	-.191	-.184	-.158	-.221	
.500	-.356	-.376	-.388	-.386	-.399	-.294	-.255	-.237	-.216	-.185	-.240	
1.000	.526	.566	.593	.621	.799	.414	.349	.510	.288	.256	.339	
1.500	2.091	2.213	2.329	2.385	2.825	2.533	1.854	1.605	1.356	1.143	1.418	
2.000	4.304	4.614	4.713	4.723	5.370	5.120	4.151	3.603	2.996	2.478	2.956	
2.500	7.158	7.727	7.787	7.696	8.511	8.165	7.051	6.307	5.263	4.304	5.007	
3.500	15.086	16.275	16.272	15.892	16.940	16.297	14.592	13.893	11.870	9.620	10.869	
4.500	26.212	28.456	28.528	28.121	29.050	27.692	25.081	25.060	21.951	17.996	20.048	
5.000	33.499	36.222	36.308	35.712	36.830	35.417	31.791	32.189	28.607	23.756	26.425	
5.250	37.515	40.529	40.626	39.870	41.042	39.658	35.522	36.179	32.351	27.004	29.999	
5.714	46.203	49.844	50.092	48.883	49.988	48.726	43.703	45.072	40.864	34.521	38.278	
5.964	50.662	55.458	55.820	53.899	55.318	54.096	48.617	50.478	46.062	39.152	43.379	
6.464	60.133	67.120	67.680	64.964	66.622	65.316	58.945	61.853	56.939	48.814	53.983	
6.964	69.807	79.007	79.965	77.056	77.272	77.398	69.959	73.964	68.402	58.913	65.012	
7.598	81.989	94.106	95.039	92.044	84.660	94.123	84.843	90.230	83.780	72.316	79.567	
7.848	86.489	99.790	100.797	97.683	87.396	100.551	90.581	96.645	89.877	77.571	85.272	
8.348	95.111	110.765	111.859	108.057	92.622	113.750	102.206	109.604	102.124	88.031	96.633	
8.848	104.845	123.043	123.981	118.674	97.545	127.993	114.440	123.116	114.980	98.569	107.997	
9.348	114.773	135.806	136.776	129.802	102.377	142.718	127.004	137.010	128.302	109.448	119.460	
9.848	124.824	148.834	149.925	141.376	107.582	157.046	139.784	151.194	142.013	120.739	131.095	
10.376	135.638	162.883	164.135	154.013	113.621	170.582	152.764	166.333	156.724	132.983	143.575	
10.626	140.869	169.702	171.052	160.251	116.939	177.256	159.017	173.618	163.857	138.913	149.560	
11.126	151.631	183.727	185.289	173.310	125.390	191.205	171.749	188.478	178.627	151.290	161.832	
11.626	162.833	198.302	200.113	187.138	137.232	205.730	184.619	203.648	194.063	164.434	174.855	
12.126	174.506	213.526	215.590	201.736	152.276	220.797	197.675	219.207	210.190	178.366	188.715	
12.720	189.229	232.524	234.973	220.120	173.358	239.345	213.499	238.315	230.320	196.024	206.491	
13.220	202.514	249.458	252.284	236.657	193.087	255.663	227.118	254.952	248.135	211.920	222.655	
14.220	231.277	286.182	289.896	272.907	236.318	290.638	255.409	289.963	286.394	246.707	258.454	
15.220	263.346	327.109	332.000	313.992	283.358	329.535	285.960	327.576	328.292	285.483	299.067	
16.220	299.230	372.576	379.053	360.209	333.892	372.641	319.957	368.304	374.070	328.307	344.600	
17.220	339.535	423.058	431.602	412.314	388.965	421.135	358.411	412.843	424.077	375.506	395.316	
18.220	384.647	479.070	490.065	470.783	449.429	475.849	402.294	461.765	478.755	427.530	451.473	
19.220	434.889	540.830	554.703	535.992	515.939	536.797	452.291	515.513	538.487	484.629	513.445	
20.220	490.176	608.447	625.768	608.399	589.156	604.395	509.233	574.418	603.706	547.006	581.252	
20.720	519.654	644.497	663.725	647.479	628.550	640.462	540.371	605.932	638.507	580.273	617.392	
21.450	565.767	701.053	723.585	710.670	692.485	698.441	591.041	656.059	693.643	632.970	674.396	
21.700	582.133	721.221	744.970	733.096	715.910	719.640	609.667	674.179	713.444	651.860	694.755	
22.200	615.353	762.173	788.388	774.776	763.769	762.911	647.779	711.083	753.561	690.081	735.908	
23.200	683.580	846.269	877.521	860.989	862.468	852.654	727.332	787.500	835.654	767.011	819.691	
24.200	753.337	933.167	969.353	949.713	965.358	947.198	810.842	867.514	920.671	847.531	905.054	

TABLE IV.-- MOMENT-COEFFICIENT SLOPE FOR MODEL I - Concluded

(b)  $\alpha = 8^\circ$ 

Model stations, x, in.	$\frac{M_X}{q_\infty \alpha}$ , in. <sup>3</sup> radian, for -										
	M = 0.248	M = 0.395	M = 0.585	M = 0.800	M = 1.000	M = 1.200	M = 1.470	M = 1.900	M = 2.700	M = 3.400	M = 4.630
0.000	0.000	0.000	0.000	0.000	0.000	0.000	0.000	0.000	0.000	0.000	0.000
.125	-.108	-.114	-.112	-.103	-.087	-.073	-.067	-.068	-.068	-.067	-.068
.250	-.293	-.311	-.310	-.299	-.249	-.201	-.182	-.182	-.180	-.176	-.180
.500	-.346	-.370	-.375	-.376	-.381	-.311	-.246	-.230	-.215	-.205	-.205
1.000	.524	.565	.581	.592	.746	.496	.340	.307	.294	.284	.286
1.500	2.064	2.209	2.258	2.285	2.624	2.497	1.812	1.575	1.362	1.258	1.225
2.000	4.215	4.516	4.561	4.619	5.057	5.142	4.045	3.555	2.989	2.716	2.609
2.500	6.975	7.483	7.525	7.618	8.100	8.299	6.925	6.254	5.228	4.716	4.488
3.500	14.567	15.639	15.651	15.882	16.325	16.595	14.539	13.952	11.712	10.456	9.948
4.500	25.463	27.257	27.630	27.781	28.176	28.673	25.314	25.281	21.699	19.739	18.728
5.000	32.436	34.723	34.808	35.584	35.742	36.302	32.187	32.611	28.379	26.039	24.893
5.250	36.277	38.868	38.933	38.876	39.841	40.425	36.008	36.723	32.172	29.605	28.349
5.714	44.568	47.850	47.946	49.127	48.543	49.251	44.480	45.946	40.806	37.810	36.380
5.964	49.276	53.362	53.411	53.739	53.721	54.486	49.605	51.559	46.076	42.842	41.337
6.464	59.157	64.807	64.717	63.891	64.708	65.449	60.384	63.358	57.094	53.329	51.627
6.964	69.293	76.503	76.234	75.023	75.095	77.292	71.872	75.904	68.695	64.314	62.348
7.598	82.204	91.360	90.828	89.063	86.122	93.725	87.393	92.858	84.230	78.926	76.509
7.848	87.071	96.964	96.347	94.298	90.189	99.963	93.396	99.543	90.395	84.706	82.097
8.348	96.630	107.887	107.020	104.085	97.895	112.588	105.658	113.289	102.851	96.355	93.293
8.848	107.025	119.877	118.707	114.357	105.412	126.079	118.570	127.648	115.844	108.412	104.697
9.348	117.677	132.234	130.871	125.179	113.292	140.005	131.867	142.472	129.301	120.861	116.346
9.848	128.857	144.844	143.321	136.449	122.123	153.867	145.338	157.710	143.209	133.683	128.265
10.376	140.366	158.439	156.782	148.745	132.546	167.689	159.086	173.920	158.161	147.425	141.078
10.626	146.086	165.027	163.309	154.814	137.976	174.548	165.734	181.748	165.424	154.069	147.243
11.126	157.892	178.593	176.751	167.516	150.049	188.961	179.370	197.917	180.495	167.810	159.939
11.626	170.248	192.707	190.771	180.947	164.687	204.013	193.286	214.363	196.283	182.232	173.348
12.126	183.214	207.432	205.433	195.130	180.338	219.651	207.513	231.406	212.795	197.359	187.574
12.720	199.843	225.832	223.780	213.013	200.247	238.944	224.862	252.359	233.428	216.335	205.650
13.220	214.043	242.259	240.176	229.104	218.107	255.927	239.899	270.639	251.721	233.256	222.011
14.220	245.870	277.933	275.868	264.410	256.952	292.145	271.530	309.128	291.061	269.871	258.125
15.220	281.713	317.710	315.871	304.462	300.379	332.080	305.831	350.483	334.221	310.221	298.891
16.220	321.754	361.867	360.486	349.572	348.691	376.401			395.126	381.506	354.637
17.220	366.425	410.925	410.255	400.422	402.765	426.024			443.616	433.344	403.318
18.220	416.061	465.142	465.529	457.489	463.139	481.585			496.370	490.146	456.661
19.220	470.803	524.786	526.491	521.061	530.161	543.435			553.790	552.249	514.915
20.220	531.171	589.911	593.377	591.650	604.317	611.908			616.235	620.097	578.334
20.720	563.343	624.536	629.076	629.698	644.050	648.604			649.500	656.273	612.078
21.450	613.595	678.648	685.149	690.918	707.438	707.711			702.153	713.404	665.274
21.700	631.499	697.911	705.142	712.173	730.399	729.252			721.103	733.908	684.305
22.200	667.888	736.956	745.687	754.074	777.252	773.194			759.646	775.496	722.853
23.200	742.507	816.786	828.692	840.037	874.037	864.340			839.386	860.963	801.732
24.200	819.094	898.437	913.721	927.650	978.958	960.564			922.681	949.643	883.033

TABLE V.- AXIAL-FORCE COEFFICIENT FOR MODEL I

 $[\alpha = 0^\circ]$ 

Model stations, x, in.	$\frac{F_x}{q_\infty}$ , sq in., for -											
	M = 0.248	M = 0.395	M = 0.585	M = 0.800	M = 1.000	M = 1.200	M = 1.470	M = 1.900	M = 2.700	M = 3.400	M = 4.630	
0.000	0.00	0.00	0.00	0.00	0.00	0.0000	0.0000	0.0000	0.0000	0.0000	0.0000	
.125	5.544	2.251	1.096	.645	.491	.421	.3717	.3310	.2964	.2924	.2856	
.250	15.396	6.201	2.979	1.705	1.276	1.085	.9430	.8308	.7356	.7196	.7018	
.500	28.070	11.205	5.292	2.924	2.122	1.723	1.4633	1.2607	1.0895	1.0499	1.0177	
1.000	44.277	17.636	8.272	4.522	3.221	2.432	1.9827	1.6290	1.3437	1.2667	1.2051	
1.500	61.783	24.600	11.514	6.225	4.431	3.302	2.6053	2.0372	1.5970	1.4671	1.3639	
2.000	81.928	32.617	15.245	8.197	5.839	4.359	3.3534	2.5239	1.8886	1.6892	1.5354	
2.500	104.70	41.686	19.466	10.517	7.496	5.621	4.2114	3.0800	2.2192	1.9376	1.7239	
3.500	158.11	62.912	29.310	15.900	11.357	8.631	6.2736	4.4055	3.0101	2.5307	2.1619	
4.500	221.82	88.026	40.777	22.092	15.814	12.205	8.7804	6.0204	3.9803	3.2642	2.7026	
5.000	257.46	101.97	47.045	25.417	18.230	14.185	10.169	6.9300	4.5309	3.7034	3.0616	
5.250	276.16	109.23	50.251	27.097	19.466	15.218	10.891	7.4076	4.8206	3.9351	3.2505	
5.714	293.76	116.03	53.208	28.640	20.607	16.180	11.572	7.8573	5.0926	4.1444	3.4068	
5.964	293.76	116.03	53.208	28.640	20.607	16.180	11.572	7.8573	5.0926	4.1444	3.4068	
6.464	293.76	116.03	53.208	28.640	20.607	16.180	11.572	7.8573	5.0926	4.1444	3.4068	
6.964	293.76	116.03	53.208	28.640	20.607	16.180	11.572	7.8573	5.0926	4.1444	3.4068	
7.598	293.76	116.03	53.208	28.640	20.607	16.180	11.572	7.8573	5.0926	4.1444	3.4068	
7.848	293.76	116.03	53.208	28.640	20.607	16.180	11.572	7.8573	5.0926	4.1444	3.4068	
8.348	293.76	116.03	53.208	28.640	20.607	16.180	11.572	7.8573	5.0926	4.1444	3.4068	
8.848	293.76	116.03	53.208	28.640	20.607	16.180	11.572	7.8573	5.0926	4.1444	3.4068	
9.348	293.76	116.03	53.208	28.640	20.607	16.180	11.572	7.8573	5.0926	4.1444	3.4068	
9.848	293.76	116.03	53.208	28.640	20.607	16.180	11.572	7.8573	5.0926	4.1444	3.4068	
10.376	304.90	120.50	55.321	29.841	21.330	16.780	11.965	8.0991	5.2113	4.1984	3.4358	
10.626	315.55	124.78	57.332	30.978	22.032	17.352	12.341	8.3299	5.3257	4.2541	3.4642	
11.126	337.43	133.52	61.428	33.280	23.547	18.527	13.114	8.8065	5.5684	4.3894	3.5278	
11.626	360.09	142.57	65.650	35.639	25.200	19.745	13.920	9.3101	5.8305	4.5519	3.6048	
12.126	383.54	151.92	70.006	38.053	26.960	20.997	14.760	9.8396	6.1108	4.7351	3.6070	
12.720	415.24	164.55	75.871	41.283	29.354	22.676	15.891	10.556	6.4950	4.9938	3.8379	
13.220	445.28	176.50	81.410	44.321	31.607	24.254	16.960	11.236	6.8631	5.2469	3.9824	
14.220	508.62	201.66	93.038	50.666	36.262	27.530	19.193	12.664	7.6477	5.7963	4.3088	
15.220	576.36	228.51	105.40	57.361	41.102	30.974	21.557	14.181	8.4908	6.3937	4.6918	
16.220	648.51	257.06	118.50	64.419	46.149	34.626	24.070	15.791	9.3894	7.3053	5.1206	
17.220	725.06	287.31	132.35	71.841	51.420	38.490	26.729	17.487	10.344	7.7165	5.5798	
18.220	805.97	319.22	146.89	79.582	56.899	42.539	29.529	19.272	11.353	8.4375	6.0697	
19.220	891.21	352.76	162.08	87.616	62.587	46.794	32.479	21.149	12.415	9.1982	6.5908	
20.220	980.69	387.82	177.83	95.816	68.427	51.256	35.588	23.120	13.520	9.9922	7.1388	
20.720	1026.90	405.83	185.81	99.879	71.245	53.550	37.188	24.135	14.086	10.399	7.4185	
21.450	1061.00	419.07	191.63	102.807	73.458	55.236	38.360	24.879	14.502	10.699	7.6234	
21.700	1061.00	419.07	191.63	102.807	73.458	55.236	38.360	24.897	14.502	10.699	7.6234	
22.200	1061.00	419.07	191.63	102.807	73.458	55.236	38.360	24.897	14.502	10.699	7.6234	
23.200	1061.00	419.07	191.63	102.807	73.458	55.236	38.360	24.897	14.502	10.699	7.6234	
24.200	1061.00	419.07	191.63	102.807	73.458	55.236	38.360	24.897	14.502	10.699	7.6234	

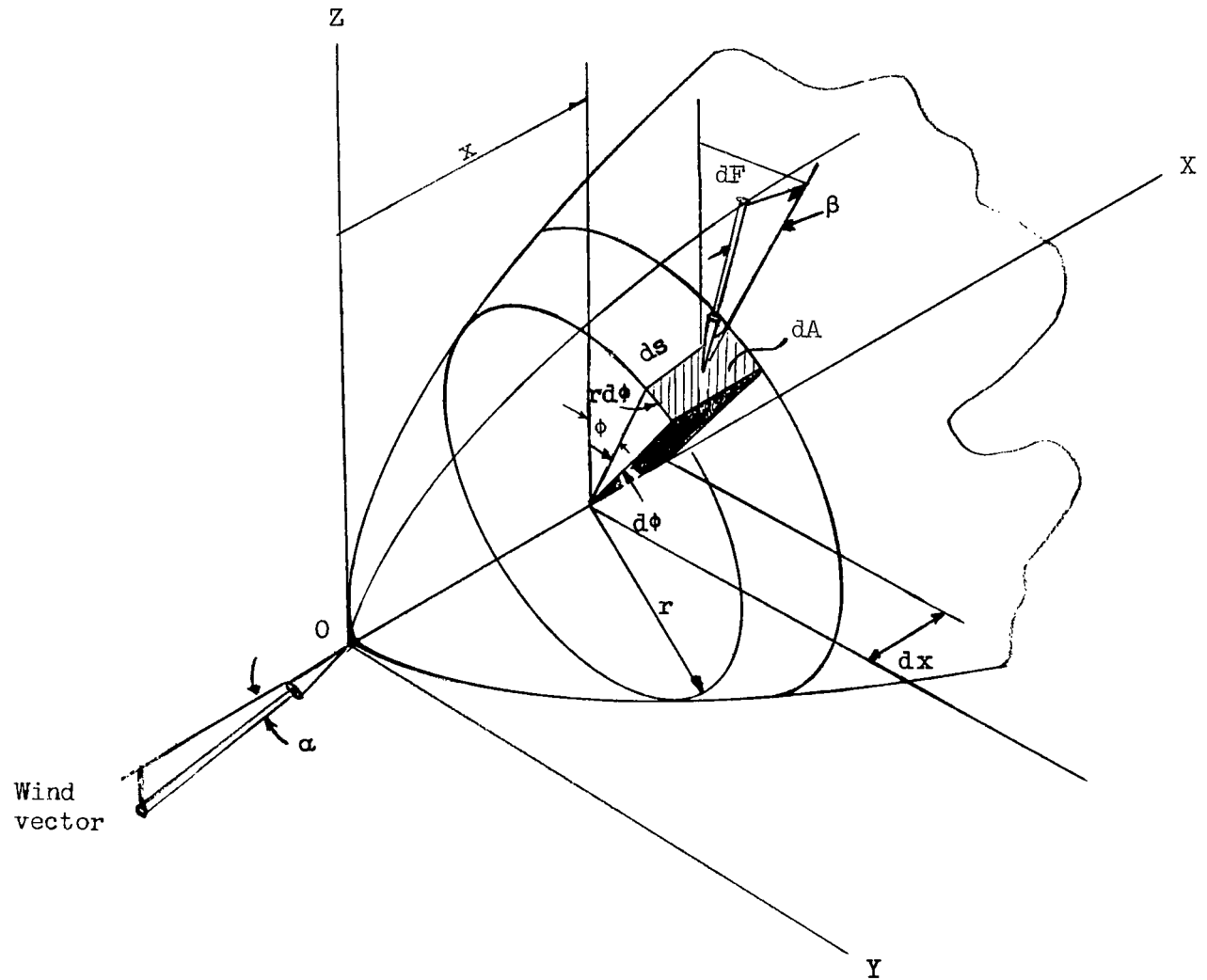


Figure 1.- Basic coordinates.

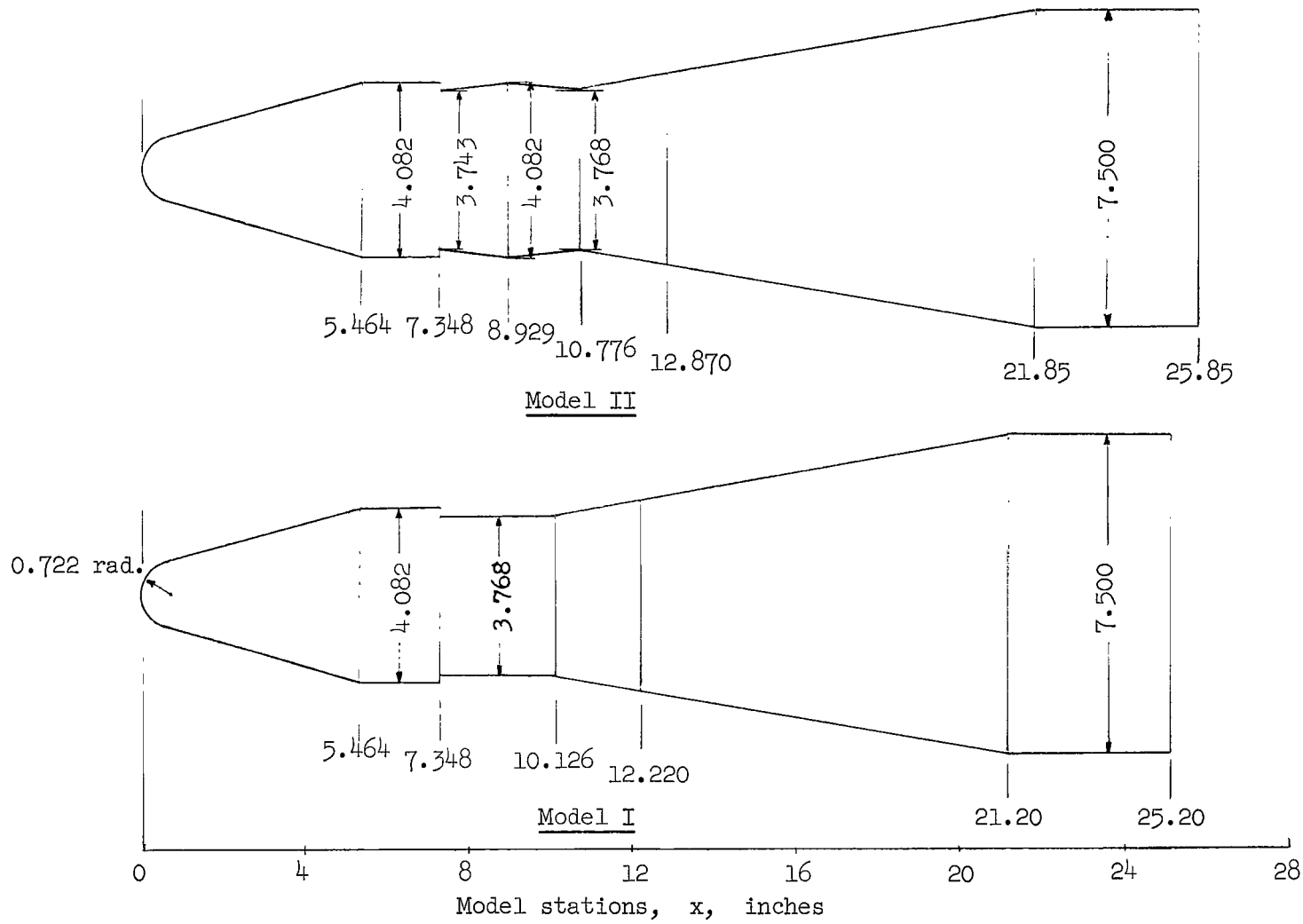


Figure 2.- Details of Project Fire configurations.

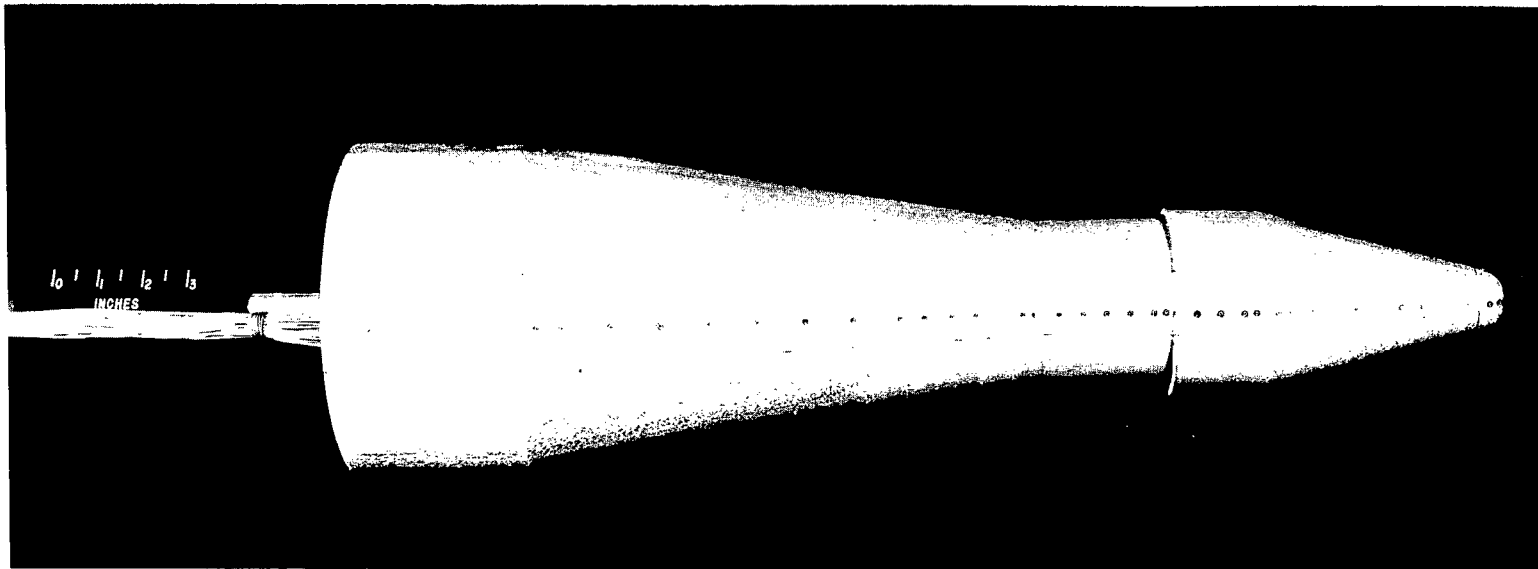


Figure 3.- Photograph of model I.

L-62-4498

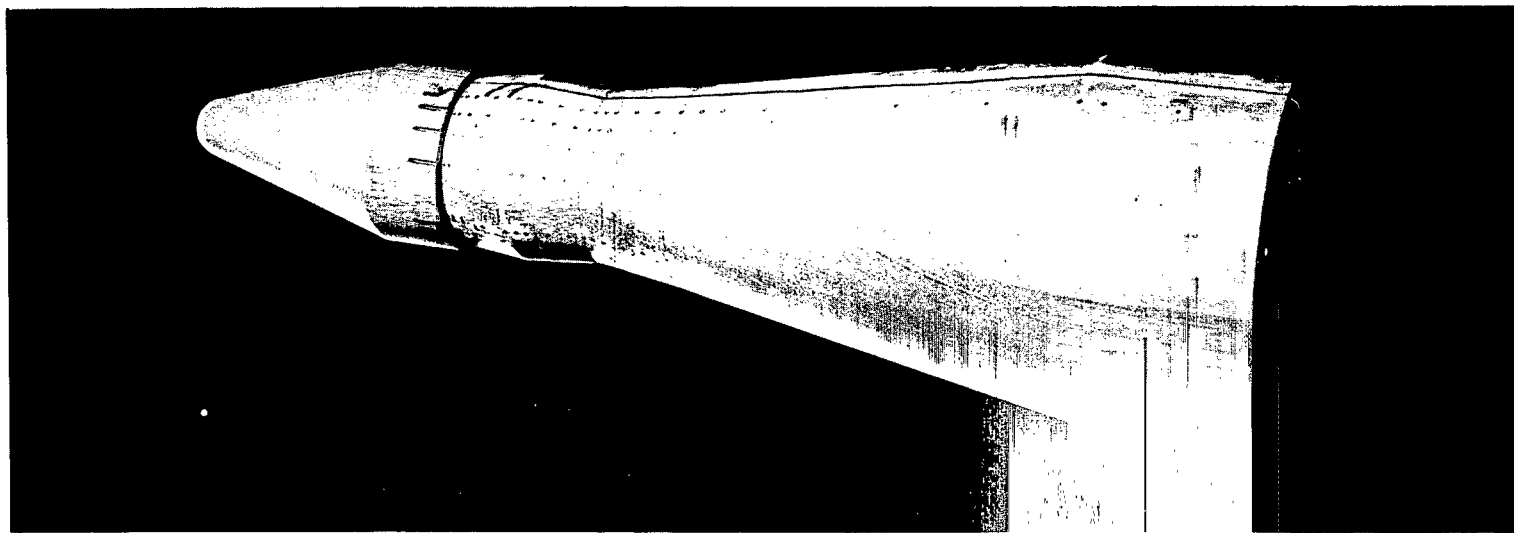


Figure 4.- Photograph of model II.

L-63-185

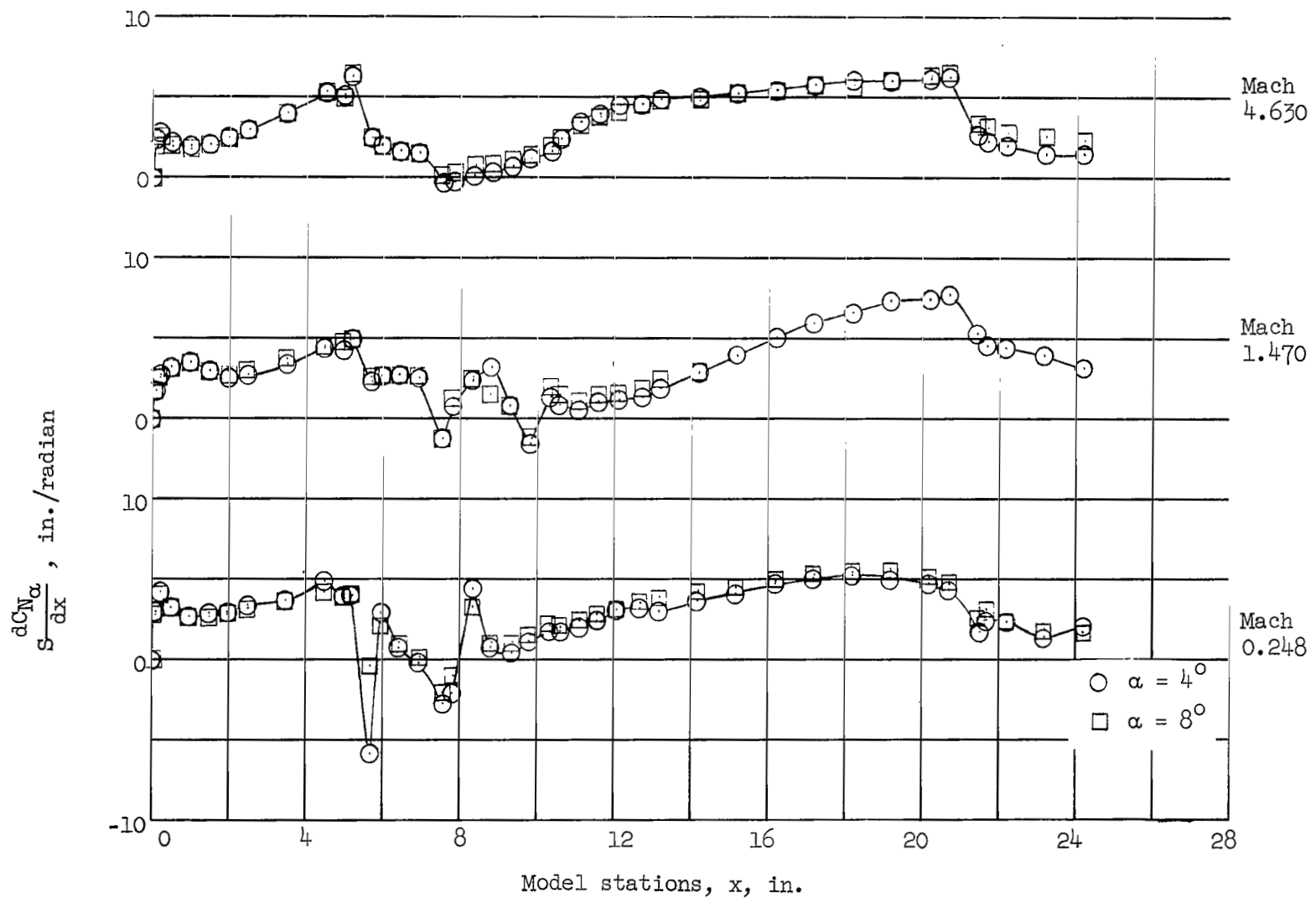


Figure 5.- Distributed normal-force-coefficient slope for a preliminary Project Fire configuration, model I.

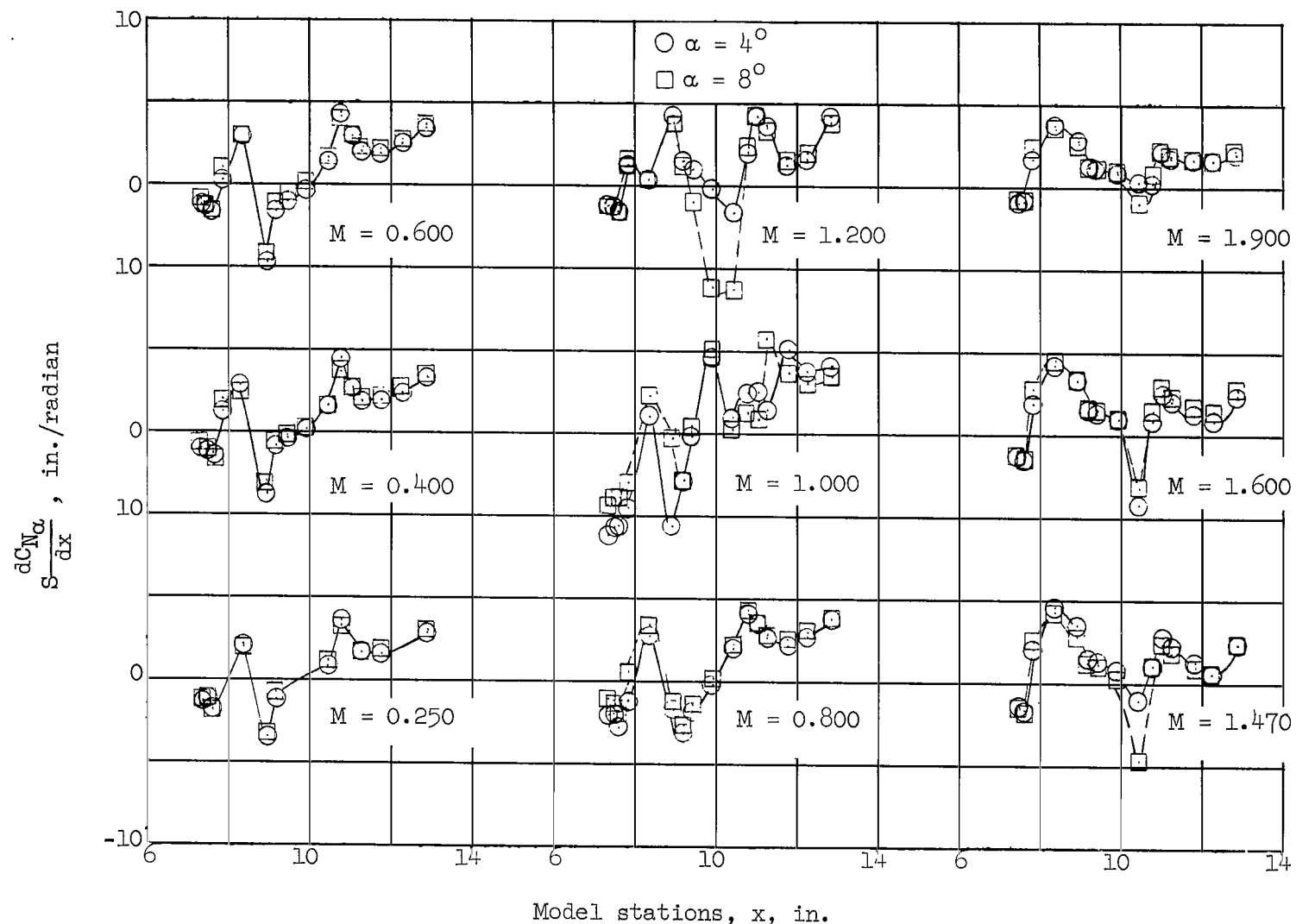


Figure 6.- Distributed normal-force-coefficient slope for the modified section of model III.

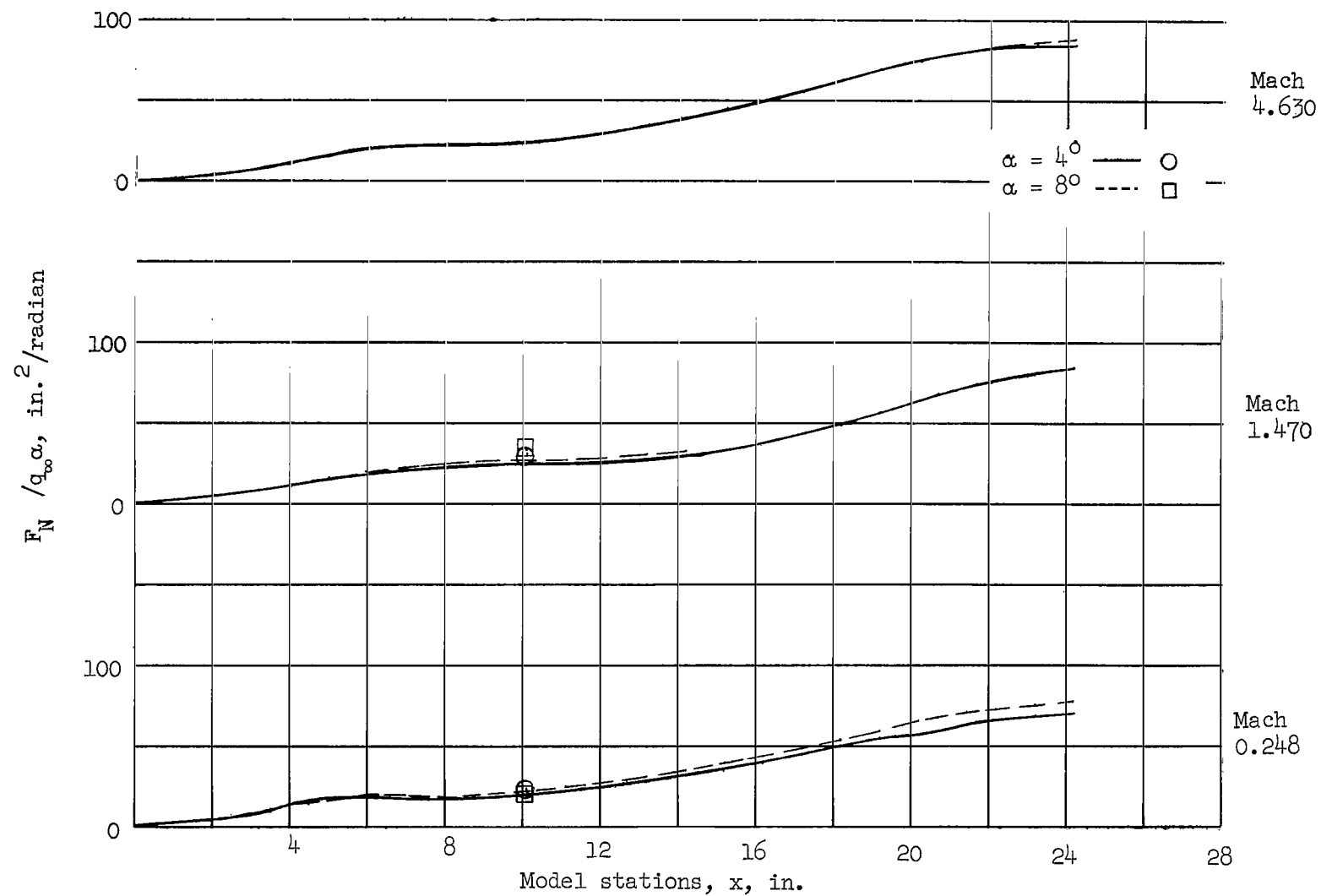


Figure 7.- Shear-coefficient slope for a preliminary Project Fire configuration, model I.

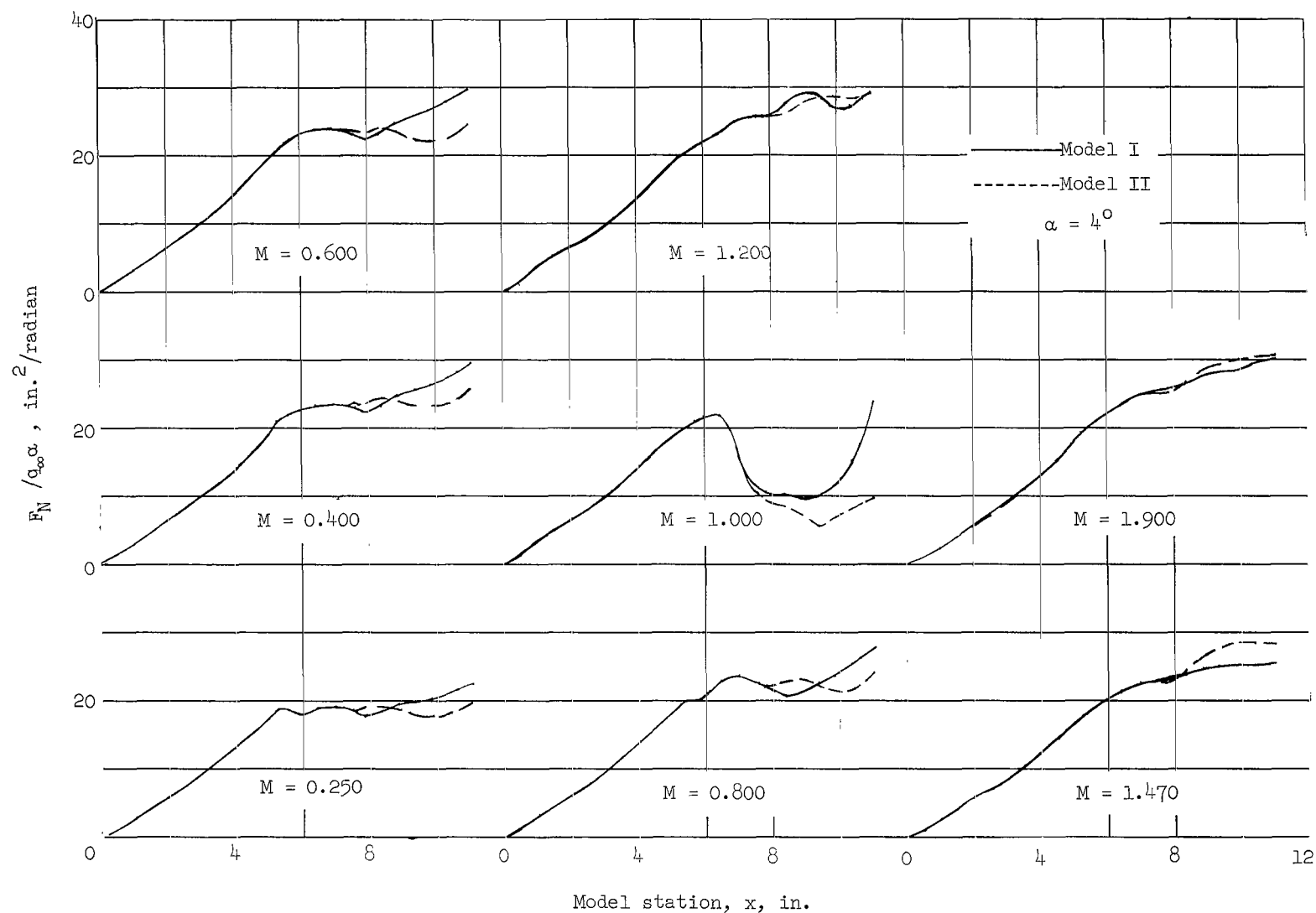


Figure 8.- Shear-coefficient slope for two versions of the Project Fire configuration.

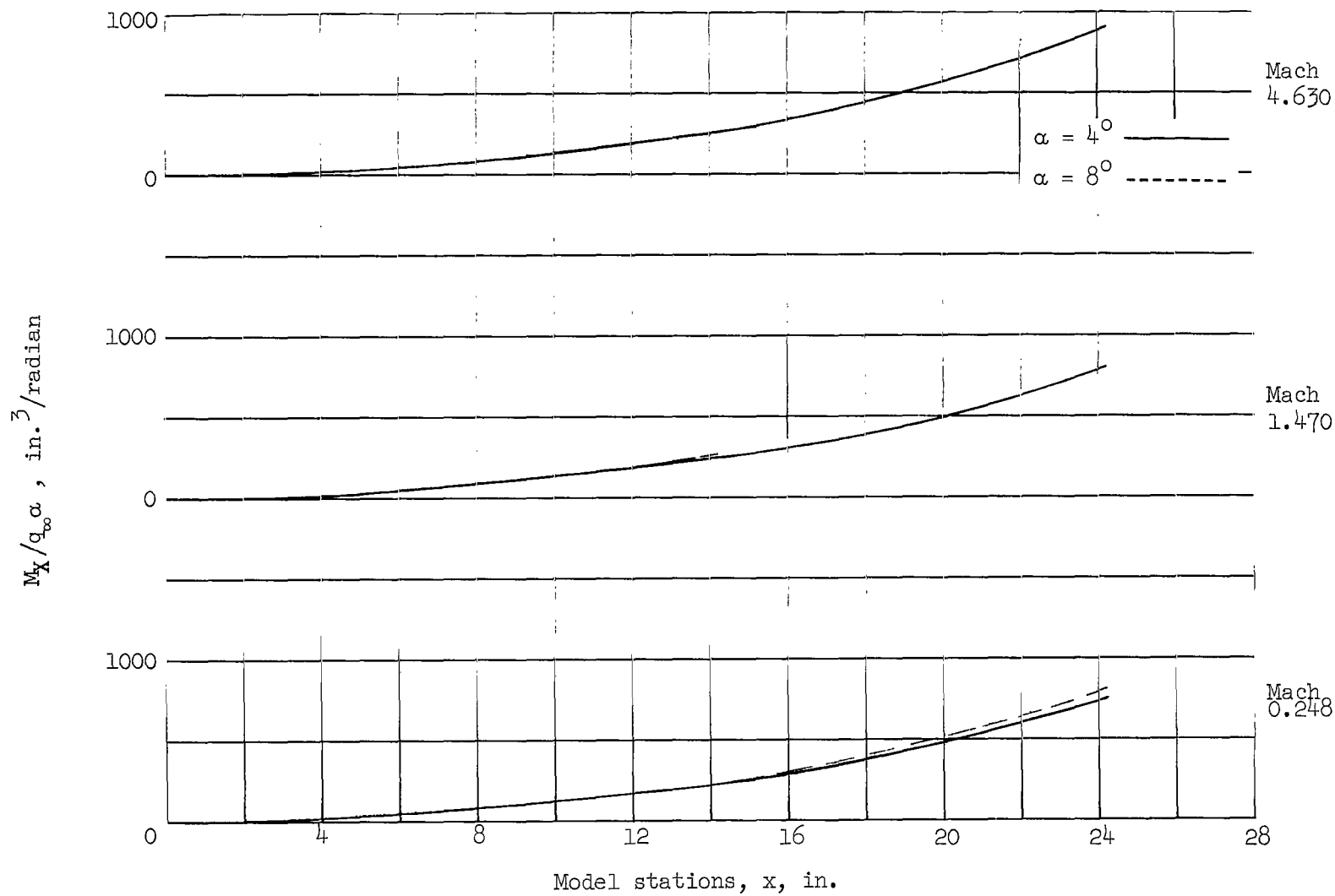


Figure 9.- Moment-coefficient slope for a preliminary Project Fire configuration, model I.

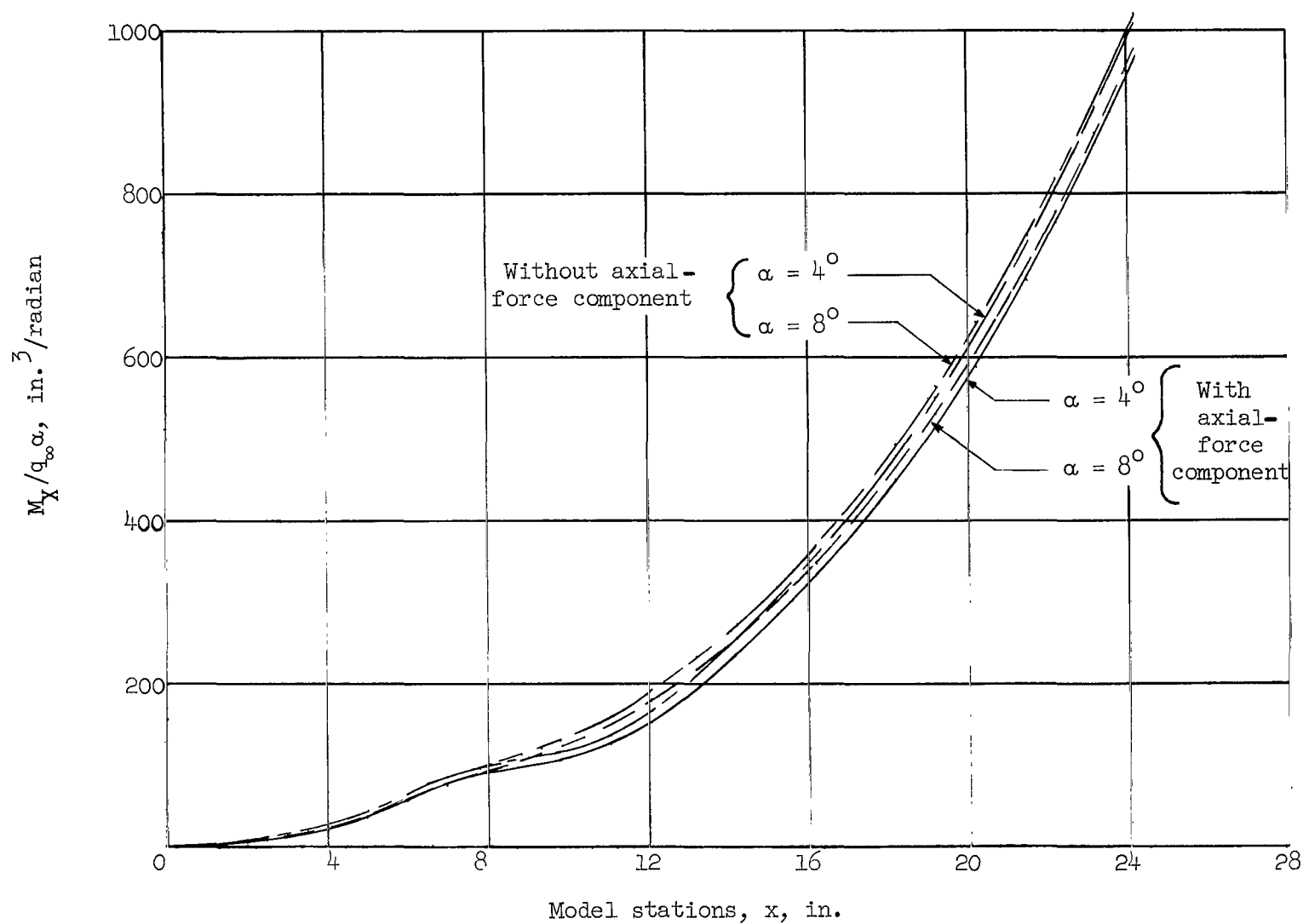


Figure 10.- Comparison of  $M_x/q_\infty \alpha$  with and without axial-force component.

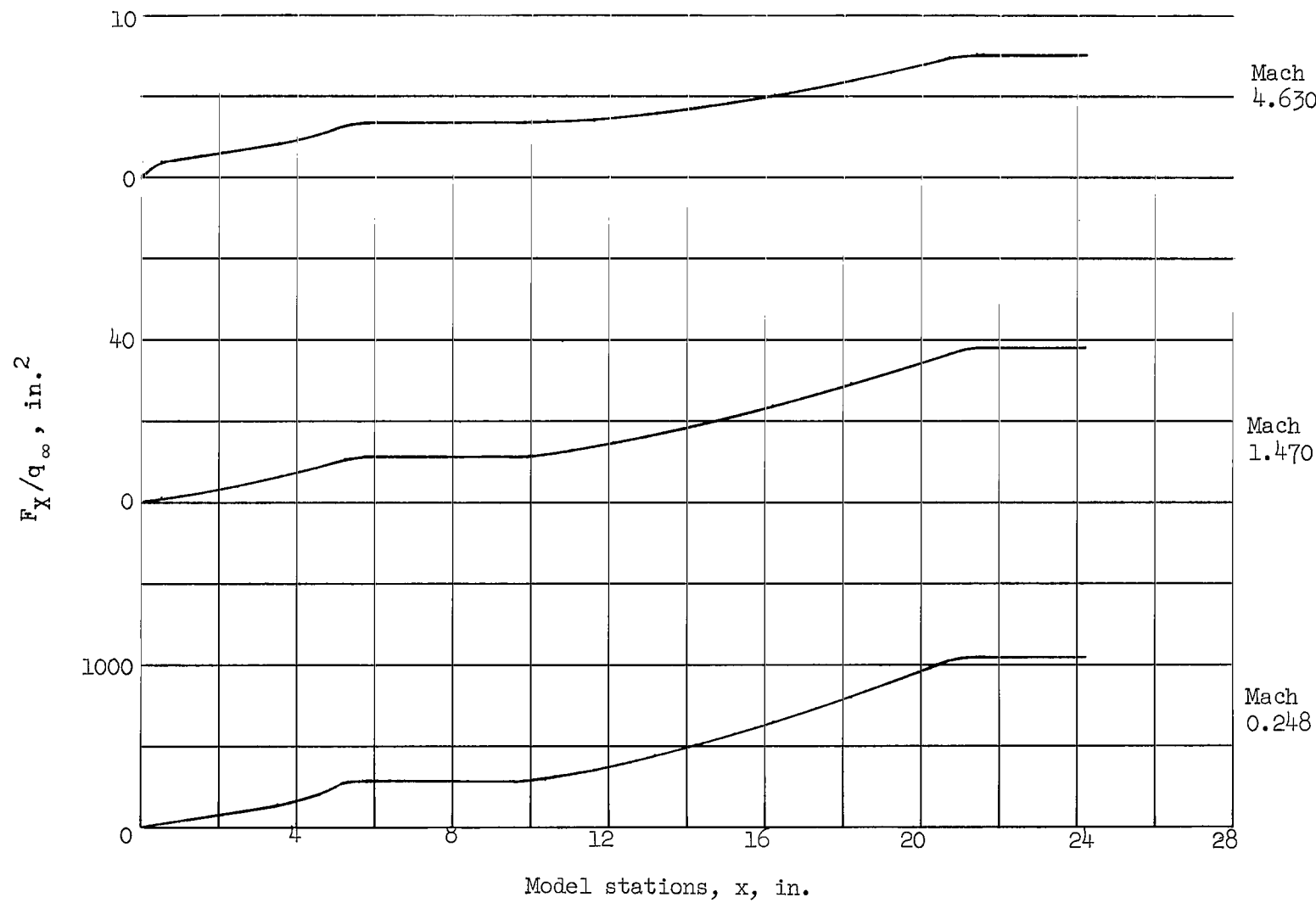


Figure 11.- Axial-force coefficient for a preliminary Project Fire configuration.  
Model I;  $\alpha = 0^\circ$ .

24/10/59

*"The aeronautical and space activities of the United States shall be conducted so as to contribute . . . to the expansion of human knowledge of phenomena in the atmosphere and space. The Administration shall provide for the widest practicable and appropriate dissemination of information concerning its activities and the results thereof."*

—NATIONAL AERONAUTICS AND SPACE ACT OF 1958

## NASA SCIENTIFIC AND TECHNICAL PUBLICATIONS

**TECHNICAL REPORTS:** Scientific and technical information considered important, complete, and a lasting contribution to existing knowledge.

**TECHNICAL NOTES:** Information less broad in scope but nevertheless of importance as a contribution to existing knowledge.

**TECHNICAL MEMORANDUMS:** Information receiving limited distribution because of preliminary data, security classification, or other reasons.

**CONTRACTOR REPORTS:** Technical information generated in connection with a NASA contract or grant and released under NASA auspices.

**TECHNICAL TRANSLATIONS:** Information published in a foreign language considered to merit NASA distribution in English.

**TECHNICAL REPRINTS:** Information derived from NASA activities and initially published in the form of journal articles.

**SPECIAL PUBLICATIONS:** Information derived from or of value to NASA activities but not necessarily reporting the results of individual NASA-programmed scientific efforts. Publications include conference proceedings, monographs, data compilations, handbooks, sourcebooks, and special bibliographies.

*Details on the availability of these publications may be obtained from:*

SCIENTIFIC AND TECHNICAL INFORMATION DIVISION  
NATIONAL AERONAUTICS AND SPACE ADMINISTRATION

Washington, D.C. 20546